



## Synthesis and properties of oxygen-bearing $c\text{-Zr}_3\text{N}_4$ and $c\text{-Hf}_3\text{N}_4$

D.A. Dzivenko<sup>a,\*</sup>, A. Zerr<sup>b</sup>, G. Miehe<sup>a</sup>, R. Riedel<sup>a</sup>

<sup>a</sup> FB Materialwissenschaft, TU Darmstadt, Petersenstr. 23, 64287 Darmstadt, Germany

<sup>b</sup> LPMTM-CNRS, Université Paris Nord, 99 av. J.B. Clement, 93430 Villetaneuse, France

### ARTICLE INFO

#### Article history:

Received 30 June 2008

Received in revised form 2 October 2008

Accepted 2 October 2008

Available online 22 November 2008

#### PACS:

61.05.cp

62.20.de

62.20.Qp

62.50.-p

64

64.30.-t

65.40.De

81.05.Je

#### Keywords:

Nitride materials

Transition metal alloys and compounds

Crystal structure

Mechanical properties

High pressure

### ABSTRACT

This paper presents our recent results on synthesis and properties of high-pressure cubic zirconium(IV)- and hafnium(IV) nitrides having  $\text{Th}_3\text{P}_4$ -type structure,  $c\text{-M}_3\text{N}_4$  ( $M = \text{Zr}$  or  $\text{Hf}$ ).  $c\text{-M}_3\text{N}_4$  were first synthesized in microscopic amounts in a laser-heated diamond anvil cell (LH-DAC) at pressures above 15 GPa and temperatures above 2500 K. Further, macroscopic amounts of  $c\text{-Hf}_3\text{N}_4$  and of a new oxygen-bearing zirconium nitride,  $c\text{-Zr}_{2.86}(\text{N}_{0.88}\text{O}_{0.12})_4$ , were synthesized at 12 GPa and about 1900 K using a multi-anvil apparatus. The lattice parameter of  $c\text{-Hf}_3\text{N}_4$  was determined to be  $a_0 = 670.2(1)$  pm. The  $a_0$  of  $c\text{-Zr}_{2.86}(\text{N}_{0.88}\text{O}_{0.12})_4$  of 675.49(1) pm was found to be slightly larger than that of  $c\text{-Zr}_3\text{N}_4$  (674.0(6) pm). The bulk moduli,  $B_0$ , of 219 GPa for  $c\text{-Zr}_{2.86}(\text{N}_{0.88}\text{O}_{0.12})_4$  and of 227 GPa for  $c\text{-Hf}_3\text{N}_4$  were obtained from compression measurements. Combining the compression and indentation data we determined for  $c\text{-Zr}_{2.86}(\text{N}_{0.88}\text{O}_{0.12})_4$  its isotropic shear modulus  $G_0 = 96$  GPa. Finally, Vickers microhardness, indentation fracture toughness and thermal expansion of  $c\text{-Zr}_{2.86}(\text{N}_{0.88}\text{O}_{0.12})_4$  were measured.

© 2008 Elsevier B.V. All rights reserved.

### 1. Introduction

The group 4 transition metal mononitrides  $\delta\text{-MN}$  (where  $M$  is  $\text{Ti}$ ,  $\text{Zr}$  or  $\text{Hf}$ ) having cubic  $\text{NaCl}$ -type structure are well known refractory materials with unique combinations of mechanical, thermal, chemical and electro-magnetic properties. They have found a broad industrial application as hard wear resistant coatings of cutting tools, corrosion and abrasion protection layers on mechanical and optical components, diffusion barriers and superconductors in microelectronics [1,2]. With respect to stoichiometric  $\text{M}_3\text{N}_4$  compounds of the group 4 elements, only orthorhombic zirconium nitride,  $o\text{-Zr}_3\text{N}_4$ , was known for a long time [3–5].

Here we review our work on synthesis, characterization and investigation of properties of novel cubic  $\text{Zr}_3\text{N}_4$  and  $\text{Hf}_3\text{N}_4$ . These nitrides were first obtained via chemical reactions of zirconium and hafnium or their mononitrides ( $\delta\text{-MN}$ ) with molecular nitro-

gen at high pressures (>15 GPa) and high temperatures (>2500 K) in a LH-DAC [6]. Examination of the structure and stoichiometry of the products using XRD and EDX revealed that the reaction products were stoichiometric nitrides  $\text{Zr}_3\text{N}_4$  and  $\text{Hf}_3\text{N}_4$  with cubic  $\text{Th}_3\text{P}_4$ -type structure (space group  $I\bar{4}3d$ , No. 220) [6]. It should be pointed out that  $c\text{-Zr}_3\text{N}_4$  and  $c\text{-Hf}_3\text{N}_4$  are the first binary nitrides with eightfold coordinated cations [6]. Preliminary compressibility measurements have indicated high bulk moduli,  $B_0$ , of about 250 GPa (with  $B'_0 = 4$ ) for both compounds thus suggesting their high hardness.

Subsequent theoretical studies of these transition metal nitrides supported the structure assignment and a low compressibility of  $c\text{-M}_3\text{N}_4$  [7–9]: The  $B_0$  values of 195–265 GPa and 215–283 GPa were predicted for  $c\text{-Zr}_3\text{N}_4$  and  $c\text{-Hf}_3\text{N}_4$ , respectively. Using these results and an empirical correlation between hardness and elastic moduli [10], Mattesini et al. [8] suggested the Vickers hardness value of about 20 GPa for the both compounds. Further interest in these materials was excited by the finding that thin films of  $c\text{-Zr}_3\text{N}_4$  are significantly harder than those of  $\delta\text{-ZrN}$  and dramatically outperform  $\delta\text{-TiN}$  (by one order of magnitude) in wear resistance by

\* Corresponding author. Tel.: +49 6151 166341; fax: +49 6151 166346.  
E-mail address: [dzivenko@materials.tu-darmstadt.de](mailto:dzivenko@materials.tu-darmstadt.de) (D.A. Dzivenko).

machining of low-carbon steels [11]. Titanium mononitride, in turn, is a well-known hard wear-resistant material which is traditionally used in mono- and multilayer coatings of cutting and milling tools because it considerably increases their service life [12,13]. The films of pure  $c\text{-Zr}_3\text{N}_4$  were prepared via the technique of physical vapour deposition (PVD) by applying a modified filtered cathodic arc method [11]. The authors were able to control the stoichiometry and the structure of the nitrides and to deposit stoichiometric  $\delta\text{-ZrN}$  or  $\text{Zr}_3\text{N}_4$  with either orthorhombic or cubic structure. These results demonstrated a great potential of  $c\text{-M}_3\text{N}_4$  for industrial application as hard wear-resistant coatings.

Very recently we succeeded in synthesis of macroscopic amounts ( $>1\text{ mm}^3$ ) of oxygen-bearing cubic zirconium(IV) nitride,  $c\text{-Zr}_{2.86}(\text{N}_{0.88}\text{O}_{0.12})_4$  [14], as well as of  $c\text{-Hf}_3\text{N}_4$  at high pressures and temperatures. The obtained materials were examined using the XRD-, TEM-, EPMA- and SEM-techniques. The results are described below. We also present accurate values for  $B_0$  of  $c\text{-Zr}_{2.86}(\text{N}_{0.88}\text{O}_{0.12})_4$  and  $c\text{-Hf}_3\text{N}_4$  derived from their equations of state (EOS),  $V(P)$ , measured on compression at RT [15,16]. Applying nanoindentation technique we obtained the reduced elastic modulus,  $E_r$ , and hardness,  $H$ , of  $c\text{-Zr}_{2.86}(\text{N}_{0.88}\text{O}_{0.12})_4$ . Combining the results for  $B_0$  and  $E_r$  we derived the shear modulus,  $G_0$ , for  $c\text{-Zr}_{2.86}(\text{N}_{0.88}\text{O}_{0.12})_4$  [15]. Hardness and fracture toughness of porous oxygen-bearing  $c\text{-Zr}_3\text{N}_4$  were determined from Vickers indentation testing. Finally, the first results on thermal expansion of  $c\text{-Zr}_{2.86}(\text{N}_{0.88}\text{O}_{0.12})_4$  from high-temperature XRD measurements will be described.

## 2. Experimental methods

The high-pressure high-temperature synthesis of macroscopic amounts of oxygen-bearing  $c\text{-Zr}_3\text{N}_4$  and of  $c\text{-Hf}_3\text{N}_4$  was performed in a multi-anvil apparatus. As a starting material we used nanocrystalline powders of nitrogen-rich zirconium and hafnium nitrides ( $\text{N}:\text{M} > 1.33$ ) having distorted NaCl-type structure [17]. The starting materials in platinum capsules were compressed to 12 GPa and heated up to 1900 K, kept at the maximum temperature for about 20 min and quenched. The recovered products were characterized using an electron probe micro-analyzer CAMECA SX-50, a scanning electron microscope Philips XL30 FEG and a TEM Philips CM20 equipped with an EDX-detector. The powder X-ray diffractograms of high-pressure nitrides were collected using a STOE STADI P diffractometer with  $\text{Mo-K}\alpha_1$  radiation.

The EOS of  $c\text{-Zr}_{2.86}(\text{N}_{0.88}\text{O}_{0.12})_4$  and  $c\text{-Hf}_3\text{N}_4$ , synthesized in a multi-anvil apparatus [14] and in a LH-DAC [6], respectively, were measured on compression at RT in a DAC to about 45 GPa. Argon was used as quasi-hydrostatic pressure medium. Pressure values were determined from the EOS of crystalline argon [18]. Specific volumes of the sample material and of argon at high pressures were derived from the EDX powder diffraction patterns measured using a polychromatic synchrotron radiation (beam-line F3 at the HasyLab, DESY, Hamburg, Germany).

Nanoindentation testing was carried out on a polished surface of the porous polycrystalline  $c\text{-Zr}_{2.86}(\text{N}_{0.88}\text{O}_{0.12})_4$  using Nanoindenter XP equipped with the continuous stiffness measurement (CSM) module [19]. Experiments were performed to two maximum loads of about 23 mN and 14 mN which corresponded to maximal indentation depths of about 260 nm and 210 nm, respectively. In the Vickers hardness measurements the loads between 0.49 N and 9.8 N were applied. Thermal expansion of  $c\text{-Zr}_{2.86}(\text{N}_{0.88}\text{O}_{0.12})_4$  was examined to 873 K using a STOE STADI P X-ray diffractometer equipped with a curved imaging plate position sensitive detector.

## 3. Results and discussion

The XRD examination of the zirconium nitride product synthesized in a multi-anvil apparatus showed only lines of a cubic phase having  $\text{Th}_3\text{P}_4$ -type structure (Fig. 1). The EPMA revealed presence of a minor amount of oxygen (mass fraction of 0.024). Since in the TEM investigations no amorphous oxidic layers were observed on the grain surfaces, we concluded that oxygen was incorporated in the crystal structure and the composition of the product could be expressed as  $\text{Zr}_{2.86}(\text{N}_{0.88}\text{O}_{0.12})_4$ . This suggested formation of an oxygen-bearing cubic zirconium(IV) nitride of the general composition  $\text{Zr}_{3-u}(\text{N}_{1-u}\text{O}_u)_4$ . Here, formation of vacancies at the cation sites required by the condition of electrical neutrality is taken into account. This supposition was verified by a

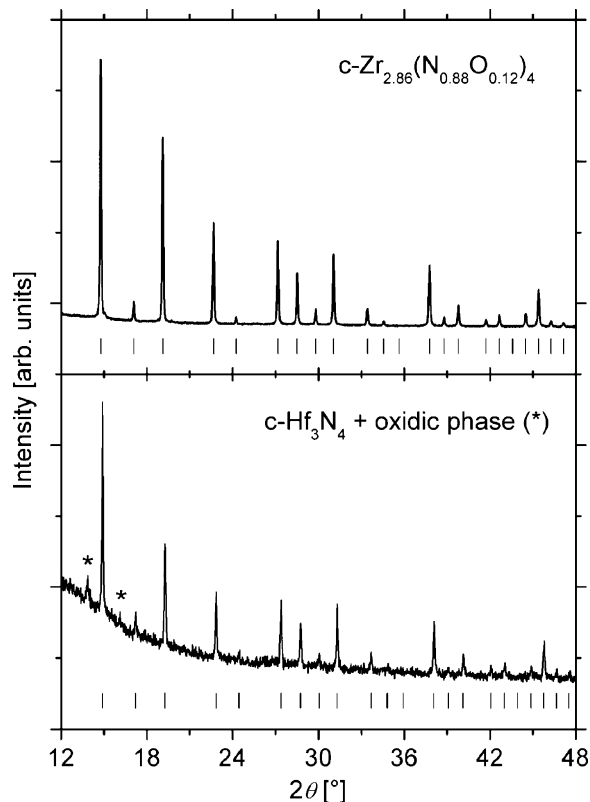


**Fig. 1.** Powder XRD patterns of  $c\text{-Zr}_{2.86}(\text{N}_{0.88}\text{O}_{0.12})_4$  (top) and  $c\text{-Hf}_3\text{N}_4$  (bottom) synthesized at 12 GPa and 1900 K in a multi-anvil apparatus. The Bragg positions of the  $\text{Th}_3\text{P}_4$ -type phases are displayed below the patterns. The asterisks denote the XRD reflexes from an oxidic impurity in the hafnium nitride sample.

full-profile Rietveld structure refinement of the XRD data (Fig. 1) [14]. The lattice parameter of  $c\text{-Zr}_{2.86}(\text{N}_{0.88}\text{O}_{0.12})_4$  was found to be  $a_0 = 675.49(1)\text{ pm}$  which is slightly larger than  $a_0 = 674.0(6)\text{ pm}$  reported earlier for  $c\text{-Zr}_3\text{N}_4$  [6]. This observation contradicts to an expected decrease of  $a_0$  due to both substitution of  $\text{N}^{3-}$  by  $\text{O}^{2-}$  anions having smaller ionic radius and formation of cation vacancies. However, recent theoretical calculations have shown that incorporation of oxygen in  $c\text{-M}_3\text{N}_4$  ( $\text{M} = \text{Zr}$  or  $\text{Hf}$ ) results in a weakening of the cation-anion bonding [20]. This leads to reduction of elastic moduli of oxygen-bearing  $c\text{-M}_3\text{N}_4$  and, on reaching of a critical oxygen concentration, to expansion of the unit cell [20]. The formation of cation vacancies, however, was not considered in the calculations.

The EPMA detected a minor amount of oxygen (mass fraction of  $\sim 0.02$ ) in hafnium nitride sample as well. However, in contrast to oxygen-bearing  $c\text{-Zr}_3\text{N}_4$ , results of XRD-, SEM- and EDX-analyses revealed the presence of a crystalline hafnium oxide or oxynitride, in addition to  $c\text{-Hf}_3\text{N}_4$ . The nature of the contaminating oxidic phase could not be determined unambiguously due to a low intensity of its XRD reflexes (Fig. 1). The lattice parameter of  $c\text{-Hf}_3\text{N}_4$  of  $a_0 = 670.2(1)\text{ pm}$  was found to be in agreement with that reported earlier ( $a_0 = 670.1(6)\text{ pm}$ ) [6]. If  $a_0$  of  $c\text{-M}_3\text{N}_4$  is influenced by substitution of nitrogen by oxygen [20], it should be recognized that, in contrast to zirconium, cubic hafnium(IV) nitride precludes oxygen incorporation in the structure. Influence of oxygen impurities on the lattice parameter and properties of  $c\text{-M}_3\text{N}_4$  could be a subject of future experimental and theoretical work.

The  $V(P)$  dependences of  $c\text{-Zr}_{2.86}(\text{N}_{0.88}\text{O}_{0.12})_4$  and  $c\text{-Hf}_3\text{N}_4$  measured at RT in a DAC to about 45 GPa [15,16] are shown in Fig. 2. From the least-square fit of the Birch-Murnaghan EOS [21] to the experimental data we obtained  $B_0 = 219(13)\text{ GPa}$ ,  $B'_0 = 4.4(10)$  and

$B_0 = 227(7)$  GPa,  $B'_0 = 5.3(6)$  for  $c\text{-Zr}_{2.86}(\text{N}_{0.88}\text{O}_{0.12})_4$  and  $c\text{-Hf}_3\text{N}_4$ , respectively. For  $B'_0$  fixed at 4 we obtained  $B_0 = 224(5)$  GPa for  $c\text{-Zr}_{2.86}(\text{N}_{0.88}\text{O}_{0.12})_4$  and  $241(2)$  GPa for  $c\text{-Hf}_3\text{N}_4$ . The theoretical predictions for  $B_0$  of  $c\text{-M}_3\text{N}_4$  [7–9] scatter around our experimental values.

SEM investigations have shown that our samples were highly porous with pore sizes of  $0.05\text{--}2\ \mu\text{m}$ . The average volume fraction porosity (VFP) was estimated to be about  $0.25\text{--}0.3$  for both zirconium- and hafnium-nitride products. Nanoindentation measurements on a polished surface of the porous  $c\text{-Zr}_{2.86}(\text{N}_{0.88}\text{O}_{0.12})_4$  gave  $E_r = 231$  GPa and  $H = 18(2)$  GPa [15]. Using the experimental values for  $B_0$  and  $E_r$  and the well-known relations between isotropic  $E_r$ ,  $E$ ,  $B$ ,  $G$ , and  $\nu$  [22] we determined for  $c\text{-Zr}_{2.86}(\text{N}_{0.88}\text{O}_{0.12})_4$   $G_0 = 96$  GPa and  $E_0 = 252$  GPa [15]. The obtained values should be considered as the lower limits since they could be altered by porosity. We were also able to perform reliable Vickers microhardness measurements for our porous  $c\text{-Zr}_{2.86}(\text{N}_{0.88}\text{O}_{0.12})_4$  and obtained  $H_V(1) = 12.0(6)$  GPa [14]. This value is similar to  $H_V(1)$  of single crystal  $\delta\text{-ZrN}$  (12.2 GPa) [23] but about 2.5 times higher than that for porous polycrystalline  $\delta\text{-ZrN}$  with the VFP of  $\sim 0.18$  [24]. Based on the known hardness-porosity relations for hard ceramic materials [24,25], we estimated the  $H_V$  value of fully dense  $c\text{-Zr}_3\text{N}_4$  to exceed 30 GPa.

For high indentation loads ( $\geq 2.94$  N) our SEM investigations revealed presence of radial cracks having their origin at the corners of the Vickers impressions. The crack lengths were used for estimation of the indentation fracture toughness,  $K_{Ic-if}$ , of  $c\text{-Zr}_{2.86}(\text{N}_{0.88}\text{O}_{0.12})_4$  according to the equations of Niihara et al. [26] and Shetty et al. [27]. The average value of  $K_{Ic-if}$  was derived to be  $3.2(3)$   $\text{MPa m}^{1/2}$  which is slightly lower than  $K_{Ic-if}$  reported for hot-isostatically pressed  $\delta\text{-MN}$  [28–30]. As above for other elasto-mechanical values, the present  $K_{Ic-if}$  is considered as the lower limit for dense  $c\text{-Zr}_3\text{N}_4$ .

In order to obtain the thermal expansion coefficient of  $c\text{-Zr}_{2.86}(\text{N}_{0.88}\text{O}_{0.12})_4$ , its XRD powder patterns were collected on heating in air to 873 K. The observed nonlinear temperature dependence of the lattice parameter of  $c\text{-Zr}_{2.86}(\text{N}_{0.88}\text{O}_{0.12})_4$  (Fig. 3) was fitted with a third order polynomial function:  $a(T) = 674.6 + 8.422 \times 10^{-6} T^2 - 2.205 \times 10^{-9} T^3$  [pm]. This dependence fulfils the boundary condition for the thermal expansion coefficient ( $\lim_{T \rightarrow 0} \alpha(T) = 0$ ) and the tendency of  $\alpha(T)$  to a

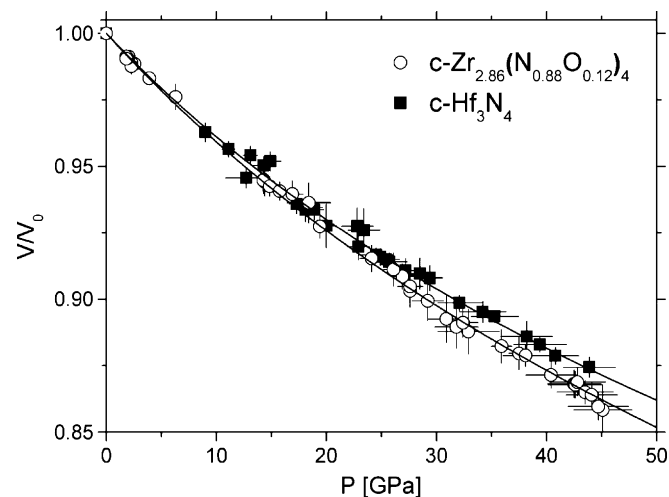


**Fig. 2.** Pressure dependences of  $V/V_0$  of  $c\text{-Zr}_{2.86}(\text{N}_{0.88}\text{O}_{0.12})_4$  (open circles) and  $c\text{-Hf}_3\text{N}_4$  (solid squares) measured at RT. Solid lines represent the least-squares fit of the third-order Birch-Murnaghan EOS to the experimental data. The fits yielded  $B_0 = 219(13)$  GPa,  $B'_0 = 4.4(10)$  and  $B_0 = 227(7)$  GPa,  $B'_0 = 5.3(6)$  for  $c\text{-Zr}_{2.86}(\text{N}_{0.88}\text{O}_{0.12})_4$  and  $c\text{-Hf}_3\text{N}_4$ , respectively.

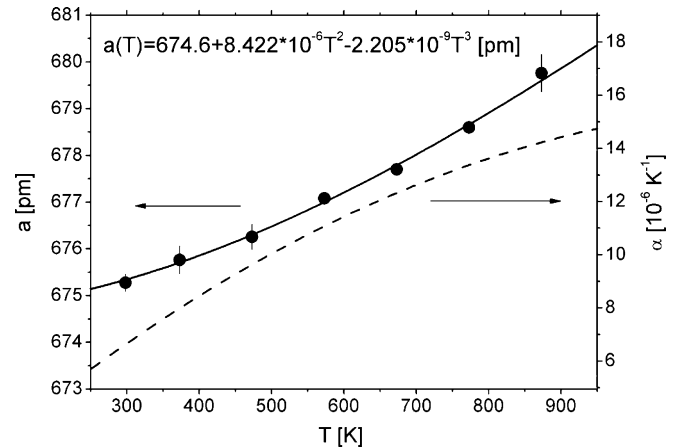


**Fig. 3.** Thermal expansion data for  $c\text{-Zr}_{2.86}(\text{N}_{0.88}\text{O}_{0.12})_4$ : Lattice parameter,  $a(T)$ , measured at elevated temperatures (solid circles) and fitted by a third order polynomial function (solid line). Linear thermal expansion coefficient,  $\alpha$ , as a function of temperature (dashed line).

constant value at high temperatures [31]. Applying this result we derived the linear thermal expansion coefficient  $\alpha(T)$  defined as  $\alpha(T) = (\partial a(T)/\partial T)/a(T)$  (Fig. 3). It can be seen from Fig. 3 that  $\alpha(T)$  increases from  $6.6 \times 10^{-6} \text{ K}^{-1}$  to  $14.2 \times 10^{-6} \text{ K}^{-1}$  in the investigated temperature region and is about twice as large as those of  $\delta\text{-ZrN}$  [32–34] and  $o\text{-Zr}_3\text{N}_4$  [5] at 900 K. Such a high  $\alpha(T)$  value of  $c\text{-Zr}_{2.86}(\text{N}_{0.88}\text{O}_{0.12})_4$  can be explained by a less symmetric interatomic potential in  $c\text{-Zr}_3\text{N}_4$  due to higher atomic coordinations when compared with  $\delta\text{-ZrN}$  and  $o\text{-Zr}_3\text{N}_4$ . It should be also mentioned that, similar to  $o\text{-Zr}_3\text{N}_4$  and zirconium oxynitrides [35],  $c\text{-Zr}_{2.86}(\text{N}_{0.88}\text{O}_{0.12})_4$  starts to oxidise in air above 773 K. The main oxidation product was found to be  $\gamma\text{-Zr}_2\text{ON}_2$  [36] which further oxidises to monoclinic  $\text{ZrO}_2$ .

## Acknowledgements

We acknowledge financial supports of the Deutsche Forschungsgemeinschaft (Bonn, Germany), the Fonds der Chemischen Industrie (Frankfurt, Germany), the Adolf-Messer-Foundation (Germany) and DESY (Hamburg, Germany). We also thank the HasyLab (at DESY) for technical support. We are grateful to V.K. Bulatov, H. Steinberg and G. Brey for multi-anvil experiments, to B. Thybusch for EPMA measurements and to E. Schweitzer and M. Göken for nanoindentation measurements.

## References

- [1] L.E. Toth, Transition Metal Carbides and Nitrides, Academic Press, New York, 1971.
- [2] W. Lengauer, in: R. Riedel (Ed.), Handbook of Ceramic Hard Materials, WILEY-VCH, Weinheim, 2000, pp. 202–252.
- [3] A. Yajima, Y. Segawa, R. Matsuzaki, Y. Saeki, Bull. Chem. Soc. Jpn. 56 (1983) 2638–2642.
- [4] R. Juza, A. Rabenau, I. Nitschke, Z. Anorg. Allg. Chem. 332 (1964) 1–4.
- [5] M. Lerch, E. Füglein, J. Wrba, Z. Anorg. Allg. Chem. 622 (1996) 367–372.
- [6] A. Zerr, G. Miehe, R. Riedel, Nat. Mater. 2 (2003) 185–189.
- [7] P. Kroll, Phys. Rev. Lett. 90 (2003) 125501.
- [8] M. Mattesini, R. Ahuja, B. Johansson, Phys. Rev. B 68 (2003) 184108.
- [9] J.E. Lowther, Physica B 358 (2005) 72–76.
- [10] D.M. Teter, MRS Bull. 23 (1998) 22–27.
- [11] M. Chhowalla, H.E. Unalan, Nat. Mater. 4 (2005) 317–322.
- [12] Y.L. Su, W.H. Kao, Wear 223 (1998) 119–130.
- [13] P. Ettmayer, W. Lengauer, Ullmann's Encyclopedia of Industrial Chemistry, Wiley-VCH, Weinheim, 1991, pp. 341.
- [14] D.A. Dzivenko, A. Zerr, V.K. Bulatov, G. Miehe, J.W. Li, B. Thybusch, J. Brötz, H. Fuess, G. Brey, R. Riedel, Adv. Mater. 19 (2007) 1869–1873.
- [15] D.A. Dzivenko, A. Zerr, E. Schweitzer, M. Göken, R. Boehler, R. Riedel, Appl. Phys. Lett. 90 (2007) 191910.

- [16] D.A. Dzivenko, A. Zerr, R. Boehler, R. Riedel, *Solid State Commun.* 139 (2006) 255–258.
- [17] J.W. Li, D.A. Dzivenko, A. Zerr, C. Fasel, Y.P. Zhou, R. Riedel, *Z. Anorg. Allg. Chem.* 631 (2005) 1449–1455.
- [18] P. Richet, J.A. Xu, H.K. Mao, *Phys. Chem. Miner.* 16 (1988) 207–211.
- [19] W.C. Oliver, G.M. Pharr, *J. Mater. Res.* 7 (1992) 1564–1583.
- [20] J.E. Lowther, *Solid State Commun.* (2008), doi:10.1016/j.ssc.2008.1009.1046.
- [21] F. Birch, *J. Geophys. Res.* 83 (1978) 1257–1268.
- [22] L.D. Landau, E.M. Lifshitz, *Course of Theoretical Physics, vol. 7: Theory of Elasticity*, vol. 7, Pergamon Press, London, 1975.
- [23] X.J. Chen, V.V. Struzhkin, Z.G. Wu, M. Somayazulu, J. Qian, S. Kung, A.N. Christensen, Y.S. Zhao, R.E. Cohen, H.K. Mao, R.J. Hemley, *Proc. Natl. Acad. Sci. U.S.A.* 102 (2005) 3198–3201.
- [24] J. Adachi, K. Kurosaki, M. Uno, S. Yamanaka, *J. Nucl. Mater.* 358 (2006) 106–110.
- [25] J. Luo, R. Stevens, *Ceram. Int.* 25 (1999) 281–286.
- [26] K. Niihara, R. Morena, D.P.H. Hasselman, *J. Mater. Sci. Lett.* 1 (1982) 13–16.
- [27] D.K. Shetty, I.G. Wright, P.N. Mincer, A.H. Clauer, *J. Mater. Sci.* 20 (1985) 1873–1882.
- [28] N. Alexandre, M. Desmaisonbrut, F. Valin, M. Boncoeur, *J. Mater. Sci.* 28 (1993) 2385–2390.
- [29] M. Desmaison-Brut, J. Montintin, F. Valin, M. Boncoeur, *J. Eur. Ceram. Soc.* 13 (1994) 379–386.
- [30] M. Moriyama, H. Aoki, Y. Kobayashi, K. Kamata, *J. Ceram. Soc. Jpn.* 101 (1993) 279–284.
- [31] H.T. Hintzen, M. Hendrix, H. Wondergem, C.M. Fang, T. Sekine, G. de With, *J. Alloys Compd.* 351 (2003) 40–42.
- [32] M. Takano, S. Tagami, K. Minato, T. Kozaki, S. Sato, *J. Alloys Compd.* 439 (2007) 215–220.
- [33] T.W. Baker, *Acta Cryst.* 11 (1958) 300–3300.
- [34] K. Aigner, W. Lengauer, D. Rafaja, P. Ettmayer, *J. Alloys Compd.* 215 (1994) 121–126.
- [35] M. Lerch, Fakultät für Chemie und Pharmazie, Bayerische Julius-Maximilians-Universität, Würzburg, 1997.
- [36] S.J. Clarke, C.W. Michie, M.J. Rosseinsky, *J. Solid State Chem.* 146 (1999) 399–405.